Two-lepton tales: Dalitz decays of heavy quarkonia

P. Colangelo,[1] F. De Fazio,[1] and R. Pinto[2]

[1]*Istituto Nazionale di Fisica Nucleare, Sezione di Bari, Via Orabona 4, 70126 Bari, Italy*
[2]*Dipartimento Interateneo di Fisica "Michelangelo Merlin", Università degli Studi di Bari, via Orabona 4, 70126 Bari, Italy*

(Received 24 January 2026; accepted 6 April 2026; published 24 April 2026)

We study the Dalitz decays of heavy quarkonia, which result from the internal virtual photon conversion into an $\ell^+\ell^-$ lepton pair. Heavy-quark symmetries allow us to establish systematic relations between transitions of different quarkonium states and to precisely determine the branching fractions for several charmonium and bottomonium decay modes. For charmonium, existing data on $\chi_{cJ}(1P) \to J/\psi \ell^+\ell^-$ and $\psi(2S) \to \chi_{cJ}(1P)\ell^+\ell^-$ enable us to determine the parameters of the transition form factors and to predict the rates of yet-unobserved modes. The Dalitz transitions of $\chi_{c1}(3872)$ are important, as they can help assessing the structure of this meson. For bottomonium, recent LHCb measurements allow us to predict the branching fractions of $\chi_{bJ}(nP) \to \Upsilon(1S)\ell^+\ell^-$ and $h_b(nP) \to \eta_b(1S)\ell^+\ell^-$ ($n = 1, 2$). We also investigate the sensitivity of heavy quarkonia Dalitz modes to the contribution of a new light vector mediator, such as the putative $X(17)$.

DOI: 10.1103/6wdr-tr4f

I. INTRODUCTION

The Dalitz decays of mesons [1], electromagnetic process where a virtual photon converts into a charged lepton pair (known as the internal photon conversion mechanism), are important probes of hadron structure. Inspection of the Review of Particle Properties [Particle Data Group (PDG)] indicates that several Dalitz modes have been observed and studied in detail for light mesons [2–4]. Conversely, only a few measurements are available in the charmonium sector and none in the bottomonium sector. Nevertheless, there is a substantial interest in the Dalitz modes of heavy quarkonia. These processes are valuable to study QCD properties, specifically the consequences of spin symmetry emerging in the heavy quark limit [5,6]. Moreover, they can aid in assessing the structure of controversial states, with $\chi_{c1}(3872)$ meson [formerly $X(3872)$] being the prime example. An additional motivation is their potential sensitivity to non-Standard-Model contributions, as the contribution of light vector mediators very feebly coupled to Standard Model (SM) particles, which are generally referred to as dark photon (γ') or dark Z. The hypothetical $X(17)$, whose existence has been invoked in connection with the ATOMKI anomaly [7], is one of such examples.

For pointlike particles, the $M' \to M\ell^+\ell^-$ decay distribution (where ℓ is a charged lepton) can be computed in terms of the radiative branching fraction $\mathcal{B}_{\rm rad}(M' \to M\gamma)$ and of a QED factor $F_{\rm QED}$ which depends on q^2, the squared lepton pair invariant mass. For extended hadrons, a transition form factor (TFF) must be included in the expression of the decay distribution,

$$\frac{d\mathcal{B}(M' \to M\ell^+\ell^-)}{dq^2} = \mathcal{B}_{\rm rad}(M' \to M\gamma)\frac{\lambda^{1/2}(m_{M'}^2, m_M^2, q^2)}{\lambda^{1/2}(m_{M'}^2, m_M^2, 0)} \times F_{\rm QED}(q^2)|f(q^2)|^2, \quad (1)$$

with λ the triangular function. $f(q^2)$ is the transition form factor normalized to $f(q^2 = 0) = 1$ [4,8]. It is sensitive to the structure of the particles involved in the decay and must be determined in a nonperturbative QCD approach or by comparing the spectrum to measurement.

For heavy quarkonia, the symmetries that emerge in the large heavy quark (HQ) mass limit establish relationships among the decay modes of different states. These symmetries allow us to utilize existing measurements to predict the rates of unobserved decays. Furthermore, the connections of the Dalitz rates to the radiative ones are useful to gaining additional information about $\chi_{c1}(3872)$ meson through Dalitz processes. The relationship involves the measured radiative branching fraction $\mathcal{B}_1 = \mathcal{B}(\chi_{c1}(3872) \to J/\psi\gamma)$, as well as $\mathcal{B}_2 = \mathcal{B}(\chi_{c1}(3872) \to \psi(2S)\gamma)$ and their ratio $\mathcal{B}_2/\mathcal{B}_1$. The availability of both the electron and muon channels doubles the set of accessible observables.

We discuss the application of the heavy quark symmetries to heavy quarkonia to determine radiative and Dalitz decay amplitudes in Sec. II, after a derivation of Eq. (1). Section III presents an analysis of charmonia and bottomonia Dalitz modes with predictions relevant for ongoing and future experimental investigations. Section IV contains a study of the potential contribution of a light new vector mediator in two specific charmonium Dalitz channels and an assessment of the precision required to achieve sensitivity to this effect. We conclude with a summary.

II. DALITZ DECAYS OF HEAVY QUARKONIA

A. Dilepton mass distribution in Dalitz decays

To apply Eq. (1) to heavy quarkonia exploiting the relation between Dalitz and radiative modes, we derive this expression in a straightforward way [4]. Consider the decay $M'(p'=m_{M'}v')\to M(p=m_M v)\ell^-(k_1)\ell^+(k_2)$ where M' and M are heavy quarkonium states of mass $m_{M'}$ and m_M and 4-velocity v' and v, respectively. The internal photon conversion amplitude

$$\begin{aligned}\mathcal{A}(M'\to M\ell^-\ell^+) &= (iee_Q)\langle M(v)|\bar{Q}\gamma^\mu Q|M'(v')\rangle \\ &\quad\times\frac{-ig_{\mu\nu}}{q^2}(-ie)\bar{u}_\ell(k_1)\gamma^\nu v_\ell(k_2) \\ &= -ie^2 e_Q\mathcal{M}^\mu\frac{g_{\mu\nu}}{q^2}L^\nu \end{aligned}\tag{2}$$

involves the matrix element $\mathcal{M}^\mu$ of the quark vector current $\mathcal{M}^\mu=\langle M(v)|\bar{Q}\gamma^\mu Q|M'(v')\rangle$, with Q the heavy quark of charge ee_Q (e is the positron charge). $q=p'-p$ is the virtual photon momentum, and L^ν is the leptonic current. The q^2 distribution for a decaying particle of spin J reads

$$\begin{aligned}&\frac{d\Gamma}{dq^2}(M'\to M\ell^-\ell^+)\\ &\quad=\frac{1}{(2J+1)}\frac{\alpha e_Q^2}{4m_{M'}^3}\lambda^{1/2}(m_{M'}^2,m_M^2,q^2)|F(q^2)|^2\\ &\qquad\times\frac{\alpha}{3\pi q^4}(2m_\ell^2+q^2)\sqrt{1-\frac{4m_\ell^2}{q^2}},\end{aligned}\tag{3}$$

with α the fine structure constant, $|F(q^2)|^2=\sum\mathcal{M}^\mu\mathcal{M}^*{}_\mu$ (the sum is over the hadron spins), and m_ℓ the lepton mass. This can be written as

$$\begin{aligned}&\frac{d\Gamma}{dq^2}(M'\to M\ell^-\ell^+)\\ &\quad=\Gamma(M'\to M\gamma)\frac{\lambda^{1/2}(m_{M'}^2,m_M^2,q^2)}{\lambda^{1/2}(m_{M'}^2,m_M^2,0)}\left|\frac{F(q^2)}{F(0)}\right|^2\\ &\qquad\times\frac{\alpha}{3\pi q^4}(2m_\ell^2+q^2)\sqrt{1-\frac{4m_\ell^2}{q^2}},\end{aligned}\tag{4}$$

where

$$\Gamma(M'\to M\gamma)=\frac{1}{(2J+1)}\frac{\alpha e_Q^2}{4m_{M'}^3}\lambda^{1/2}(m_{M'}^2,m_M^2,0)|F(0)|^2\tag{5}$$

is the radiative decay width. Equation (1) is obtained defining $f(q^2)=\frac{F(q^2)}{F(0)}$ and

$$F_{\mathrm{QED}}(q^2)=\frac{\alpha}{3\pi q^4}(2m_\ell^2+q^2)\sqrt{1-\frac{4m_\ell^2}{q^2}}.\tag{6}$$

The relationship between Dalitz modes and radiative modes is useful to extract information on Dalitz processes using existing results on radiative modes, and vice versa. For heavy quarkonia, the analysis is further enhanced by exploiting the symmetries arising in QCD in the heavy quark limit.[1]

B. Heavy quark symmetries and radiative decays of quarkonia

In the heavy quark limit, the radiative decays of quarkonia, important for the description of the Dalitz modes as witnessed by Eq. (1), can be described in an effective Lagrangian approach. The effective Lagrangian is built on the basis of the symmetries holding in QCD in the infinite mass limit $m_Q\to\infty$ (the heavy quark HQ limit) [6].

The QCD Lagrangian in the HQ limit is obtained defining the field $h_v(x)=e^{im_Q v\cdot x}P_+Q(x)$, where Q is the HQ field in QCD and v is the heavy quark 4-velocity. The field h_v is obtained through the velocity projector $P_+=\frac{1+\not{v}}{2}$, $h_v=P_+Q$, and satisfies the condition $\not{v}h_v=h_v$. The QCD Lagrangian for the heavy quark Q can be written in terms of h_v as an expansion in m_Q^{-1}, with the leading term in the expansion (the heavy quark effective theory (HQET) Lagrangian),

$$\mathcal{L}_{\mathrm{HQET}}=\bar{h}_v iv\cdot Dh_v.\tag{7}$$

D is the QCD covariant derivative. For N_f heavy flavors, the Lagrangian (7) is invariant under $SU(2N_f)$ spin/flavor rotations. The next-to-leading terms in the heavy quark expansion can be systematically included, and they break the spin/flavor symmetry. The subleading operators are suppressed by powers of k/m_Q, where k is a residual momentum of $\mathcal{O}(\Lambda_{\mathrm{QCD}})$ introduced to take into account that the HQ is off shell writing its momentum as $p=m_Q v+k$. At $\mathcal{O}(1/m_Q)$, two operators arise:

$$\mathcal{L}^{(1)}=\frac{1}{2m_Q}\bar{h}_v(i\not{D}_\perp)^2h_v+\frac{1}{2m_Q}\bar{h}_v\frac{g_s\sigma_{\alpha\beta}G^{\alpha\beta}}{2}h_v,\tag{8}$$

[1]Dalitz decays of open charm mesons are discussed in Ref. [9].

the HQ kinetic energy operator due to the residual momentum k, and the chromomagnetic operator due to coupling of the HQ spin to the gluon field. Both the operators break the flavor symmetry, and the second one also breaks the heavy quark spin symmetry. Such properties have extensively been applied in the analysis of hadrons comprising a single heavy quark [5]. However, for systems comprising a heavy quark-antiquark pair, the heavy quarkonia, the flavor symmetry cannot be exploited even at the leading order in the expansion [10]. The reason is that for two heavy quarks with the same velocity diagrams describing their gluon exchanges are affected by infrared divergences that can be regulated going beyond the leading order in the HQ expansion, including of the kinetic energy operator. Nevertheless, the HQ spin symmetry still survives.

A consequence of the spin symmetry is that in the heavy quark limit hadrons differing for the HQ spin orientation are degenerate, and they can be treated in a unified way collecting them in spin multiplets. The degeneracy is broken starting from terms of $\mathcal{O}(1/m_Q)$, i.e., from the chromomagnetic operator. Heavy-light mesons can be organized in spin doublets, the two states obtained in correspondence to the two orientations of the spin of the heavy quark. For $Q\bar{Q}$ systems, both the spin of the heavy quark and of the heavy antiquark can be rotated, and the spin multiplets contain a number of states which depends on the relative orbital angular momentum L between the heavy quarks. We are interested in $L=0$ (S-wave) states, that can be organized in a spin doublet, and $L=1$ (P-wave) states organized in a spin quartet. The two multiplets can be represented as follows [11,12]:

(i) $L=0$ *doublet.*

$$J=\frac{1+\slashed{v}}{2}[H_1^\mu\gamma_\mu-H_0\gamma_5]\frac{1-\slashed{v}}{2}. \tag{9}$$

(ii) $L=1$ *quartet.*

$$J^\mu=\frac{1+\slashed{v}}{2}\left\{H_2^{\mu\alpha}\gamma_\alpha+\frac{1}{\sqrt{2}}\epsilon^{\mu\alpha\beta\gamma}v_\alpha\gamma_\beta H_{1\gamma}+\frac{1}{\sqrt{3}}(\gamma^\mu-v^\mu)H_0+K_1^\mu\gamma_5\right\}\frac{1-\slashed{v}}{2}. \tag{10}$$

v^μ is the heavy quark four-velocity, with the transversality condition $v_\mu J^\mu=0$. H_A and K_A are the effective fields for the members of the multiplets with total spin $J=A$.

In terms of the spin multiplets, effective Lagrangians can be constructed to describe the heavy quarkonium phenomenology. We use the effective Lagrangian describing radiative decays of heavy quarkonia in the soft-gluon-exchange approximation [13]. The electric dipole radiative transitions of members of P-wave multiplet to members of the S-wave doublet, with the orbital angular momentum of the decaying and of the produced quarkonium differing by $\Delta L=1$, are described by the effective Lagrangian

$$\mathcal{L}_{nP\leftrightarrow mS}=\delta_Q^{nPmS}\mathrm{Tr}[\bar{J}(mS)J_\mu(nP)]v_\nu F^{\mu\nu}+\mathrm{H.c.}, \tag{11}$$

where n and m are radial quantum numbers, $\bar{J}=\gamma^0J^\dagger\gamma^0$, and $F^{\mu\nu}$ is the electromagnetic field strength tensor. δ_Q^{nPmS} indicates the single coupling governing the transitions from the quartet of P states with radial quantum number n to the doublet of S states with radial quantum number m, for mesons comprising the heavy quark Q. This Lagrangian is invariant under parity (P), charge conjugation (C), and time reversal (T) transformations,

$$J^{\mu_1\cdots\mu_L}\xrightarrow{P}\gamma^0J_{\mu_1\ldots\mu_L}\gamma^0 \tag{12}$$

$$J^{\mu_1\cdots\mu_L}\xrightarrow{C}(-1)^{L+1}C[J^{\mu_1\cdots\mu_L}]^TC \tag{13}$$

$$J^{\mu_1\cdots\mu_L}\xrightarrow{T}-TJ_{\mu_1\ldots\mu_L}T^{-1}, \tag{14}$$

where $C=i\gamma^2\gamma^0$ and $T=i\gamma^1\gamma^3$. Moreover, the Lagrangian (11) is invariant under heavy quark spin transformations, that for a generic L-wave multiplet $J^{\mu_1\cdots\mu_L}$ read

$$J^{\mu_1\cdots\mu_L}\xrightarrow{SU(2)_{S_h}}SJ^{\mu_1\cdots\mu_L}S'^\dagger. \tag{15}$$

S and S' belong to $SU(2)_{S_h}$, the group of heavy quark spin rotations, and satisfy the relations $[S,\slashed{v}]=[S',\slashed{v}]=0$. The spin symmetry implies that the single coupling constant δ_Q^{nPmS} describes all transitions between $Q\bar{Q}$ states in a nP multiplet to the states in a mS doublet [13–15]. The expressions of the corresponding decay widths are collected in the Appendix.

The $\Delta L=0$ magnetic dipole transitions among members of the S-wave doublets are instead governed by the effective Lagrangian

$$\mathcal{L}_{nS\leftrightarrow mS}=\delta_Q^{nSmS}\mathrm{Tr}[\bar{J}(mS)\sigma_{\mu\nu}J(nS)]F^{\mu\nu}+\mathrm{H.c.}, \tag{16}$$

which is invariant under P, C, T transformations but violates the spin symmetry [16]. The resulting expression of the decay width [15] is also reported in the Appendix.

The effective Lagrangians (11) and (16) can be exploited to analyze the radiative heavy quarkonia transitions, to verify the accuracy of the HQ limit, to determine the couplings from the measured radiative rates, and to predict unmeasured decay widths [15]. They can also be used to get information on the structure of debated states. For example, the comparison of the computed radiative decay rates $\chi_{c1}(3872)\to\psi(1S,2S)\gamma$ with measurements supports the identification of $\chi_{c1}(3872)$ as $\chi_{c1}(2P)$ [15].

TABLE I. Measured branching fractions of radiative and Dalitz decays of charmonium and bottomonium states [2].

$M' \to M$	$\mathcal{B}(M' \to M\gamma)$	$\mathcal{B}(M' \to M\mu^+\mu^-)$	$\mathcal{B}(M' \to Me^+e^-)$
$\chi_{c0}(1P) \to J/\psi$	$(1.41 \pm 0.09) \times 10^{-2}$	$<1.9 \times 10^{-5}$	$(1.34 \pm 0.30) \times 10^{-4}$
$\chi_{c1}(1P) \to J/\psi$	$(34.3 \pm 1.3) \times 10^{-2}$	$(2.33 \pm 0.29) \times 10^{-4}$	$(3.46 \pm 0.24) \times 10^{-3}$
$\chi_{c2}(1P) \to J/\psi$	$(19.5 \pm 0.7) \times 10^{-2}$	$(2.07 \pm 0.34) \times 10^{-4}$	$(2.20 \pm 0.15) \times 10^{-3}$
$h_c(1P) \to \eta_c$	$(60 \pm 4) \times 10^{-2}$		
$\psi(2S) \to \chi_{c0}(1P)$	$(9.75 \pm 0.22) \times 10^{-2}$		$(1.05 \pm 0.25) \times 10^{-3}$
$\psi(2S) \to \chi_{c1}(1P)$	$(9.75 \pm 0.27) \times 10^{-2}$		$(8.5 \pm 0.7) \times 10^{-4}$
$\psi(2S) \to \chi_{c2}(1P)$	$(9.38 \pm 0.23) \times 10^{-2}$		$(6.8 \pm 0.8) \times 10^{-4}$
$\chi_{c1}(3872) \to J/\psi$	$(7.8 \pm 2.9) \times 10^{-3}$		
$\chi_{b0}(1P) \to \Upsilon(1S)$	$(1.94 \pm 0.27) \times 10^{-2}$		
$\chi_{b1}(1P) \to \Upsilon(1S)$	$(35.2 \pm 2.0) \times 10^{-2}$		
$\chi_{b2}(1P) \to \Upsilon(1S)$	$(18.0 \pm 1.0) \times 10^{-2}$		
$h_b(1P) \to \eta_b(1S)$	$(52^{+6}_{-5}) \times 10^{-2}$		
$\chi_{b0}(2P) \to \Upsilon(1S)$	$(3.8 \pm 1.7) \times 10^{-3}$		
$\chi_{b1}(2P) \to \Upsilon(1S)$	$(9.9 \pm 1.0) \times 10^{-2}$		
$\chi_{b2}(2P) \to \Upsilon(1S)$	$(6.6 \pm 0.8) \times 10^{-2}$		
$h_b(2P) \to \eta_b(1S)$	$(22 \pm 5) \times 10^{-2}$		

The framework based on spin symmetry can also be applied to the heavy quarkonium Dalitz modes.[2]

III. HEAVY QUARKONIUM DALITZ MODES

The $L = 0$ charmonium and bottomonium spin doublets are $(\eta_c(nS), \psi(nS))$ and $(\eta_b(nS), \Upsilon(nS))$, with $J^{PC} = (0^{-+}, 1^{--})$ and radial quantum number n. For $L = 1$, the spin multiplets comprise four states $(\chi_{c(b)0}, \chi_{c(b)1}, \chi_{c(b)2}, h_{c(b)})$ with $J^{PC} = (0^{++}, 1^{++}, 2^{++}, 1^{+-})$. The available data quoted in Ref. [2] for the radiative and Dalitz branching ratios are collected in Table I. Only in a few cases, the rates of both channels are known. The Dalitz branching ratios are not known for most modes; in particular, no measurement is available for bottomonium, even though some processes have been observed. In our analysis, we systematically make use of Eq. (1) relating the Dalitz decay distribution and the radiative branching fraction.

A. Charmonium $1P \to 1S$ Dalitz decays

The transitions from the charmonium $1P$ quartet to the $1S$ doublet, for which more abundant data are available, can be used to verify the results based on the heavy quark limit and to predict the branching fractions of unmeasured Dalitz modes. The missing information is about the transition form factor $f(q^2)$ that should be computed by nonperturbative QCD methods or using models [19]. An alternative approach, that we follow here, is to bound the TFF using data. Inspired by vector meson dominance arguments, we choose a simple pole parametrization

$$f(q^2) = \frac{1}{1 - \frac{q^2}{a^2}}, \tag{17}$$

which involves the mass parameter a. We assume this form in the full kinematical range of the momentum transferred to the lepton pair, $4m_\ell^2 \le q^2 \le (m_{M'} - m_M)^2$. Considering that the range of q^2 is quite narrow, the parameter a should be regarded as an effective quantity describing the slope of the transition form factor in the kinematical region accessible in Dalitz decays, rather than as the mass of a physical vector resonance.

Integrating the distribution $\frac{d\mathcal{B}}{dq^2}$ in (1), one obtains the Dalitz branching fraction depending on $\mathcal{B}_{\rm rad}$ and on the mass parameter a. The linear dependence on the radiative $\mathcal{B}_{\rm rad}$ gives the excursion for the Dalitz branching ratio: $\mathcal{B}_{\rm min}(M' \to M\ell^+\ell^-) = \mathcal{B}(a, \mathcal{B}_{\rm rad} - \Delta\mathcal{B}_{\rm rad})$, $\mathcal{B}_{\rm max}(M' \to M\ell^+\ell^-) = \mathcal{B}(a, \mathcal{B}_{\rm rad} + \Delta\mathcal{B}_{\rm rad})$, with $\Delta\mathcal{B}_{\rm rad}$ the error on $\mathcal{B}_{\rm rad}$.

The radiative widths computed using the effective Lagrangian (16) and collected in the Appendix, when compared to measurement, confirm that the single coupling δ_{1P1S} governs the $1P \to 1S$ transitions for all members of the initial quartet decaying to states in the final doublet [15]. In the heavy quark limit, the matrix elements of the current $\bar{Q}\Gamma Q$ (with Γ a Dirac matrix) between two quarkonium states for q^2 close to $q^2_{\rm max}$ can be related [11]. Such relations can be extended to the full kinematic range for the narrow phase space of the Dalitz decays to muons. Moreover, in the HQ limit, the mass splitting among the states belonging the various multiplets vanishes. The consequence is that the mass parameter a in (17) is the same for all $1P \to 1S$ transitions.

The value of a can be obtained from data. For the transitions $\chi_{c1}(1P) \to J/\psi$ and $\chi_{c2}(1P) \to J/\psi$, both the

[2]The radiative decay modes of $h_{c,b}(1P)$ and $\chi_{c1}(1P)$ are analyzed by lattice QCD in Refs. [17,18].

radiative and the Dalitz branching fractions are measured, and a is constrained requiring that the range $[\mathcal{B}_{\rm min}(M' \to M\ell^+\ell^-), \mathcal{B}_{\rm max}(M' \to M\ell^+\ell^-)]$ overlaps with the experimental range in Table I. The obtained intervals are further restricted minimizing $\chi^2 = (\mathcal{B}(a) - \mathcal{B}_{\rm exp})^2/\sigma^2_{\rm exp}$, with $\mathcal{B}(a)$ the prediction for $\mathcal{B}(M' \to M\mu^+\mu^-)$ obtained for the central value of the radiative $\mathcal{B}_{\rm rad}$, $\mathcal{B}_{\rm exp}$ and $\sigma_{\rm exp}$ the Dalitz branching fraction and error in Table I. We use the meson masses quoted in Ref. [2]. From the mode $\chi_{c1}(1P) \to J/\psi\mu^+\mu^-$, we obtain $a_{c1} = 0.83^{+0.17}_{-0.11}$ GeV; from $\chi_{c2}(1P) \to J/\psi\mu^+\mu^-$, we have $a_{c2} = 0.71^{+0.13}_{-0.07}$ GeV. As expected, the pole mass parameters in the two modes are close to each other. In correspondence to a_{c1} and a_{c2}, the computed branching fractions of the muon and electron modes are

$$\mathcal{B}(\chi_{c1}(1P) \to J/\psi\mu^+\mu^-(e^+e^-)) = (2.34 \pm 0.10) \times 10^{-4}((3.06 \pm 0.12) \times 10^{-3}) \quad (18)$$

$$\mathcal{B}(\chi_{c2}(1P) \to J/\psi\mu^+\mu^-(e^+e^-)) = (2.06 \pm 0.10) \times 10^{-4}((1.83 \pm 0.08) \times 10^{-3}). \quad (19)$$

Because of the larger phase space for the dielectron channel, the extension of the HQ limit to the whole kinematical range is expected to produce a less satisfactory agreement with measurements in case of electrons. Using together the measured $\mathcal{B}(\chi_{c1}(1P) \to J/\psi\mu^+\mu^-)$ and $\mathcal{B}(\chi_{c2}(1P) \to J/\psi\mu^+\mu^-)$, we obtain

$$a_c = 0.77 \pm 0.10 \text{ GeV}, \quad (20)$$

the value we use for all $1P \to 1S$ transitions.

The computed branching fractions are collected in Table II; some of them are predictions for unobserved $1P \to 1S$ charmonium modes. The uncertainties quoted in Table II are mainly due to the errors for the branching ratios of the radiative decays, which cancel out in the ratios between the muonic and the electronic decay rates. For this reason, in Table II, we do not quote the error for $\frac{\mathcal{B}(M' \to M\mu^+\mu^-)}{\mathcal{B}(M' \to Me^+e^-)}$. The BESIII measurements $\frac{\mathcal{B}(\chi_{c1} \to J/\psi\mu^+\mu^-)}{\mathcal{B}(\chi_{c1} \to J/\psi e^+e^-)} = (6.73 \pm 0.51 \pm 0.50) \times 10^{-2}$, $\frac{\mathcal{B}(\chi_{c2} \to J/\psi\mu^+\mu^-)}{\mathcal{B}(\chi_{c2} \to J/\psi e^+e^-)} = (9.40 \pm 0.79 \pm 1.15) \times 10^{-2}$, and the upper bound $\frac{\mathcal{B}(\chi_{c0} \to J/\psi\mu^+\mu^-)}{\mathcal{B}(\chi_{c0} \to J/\psi e^+e^-)} < 14 \times 10^{-2}$ (at 90% C.L.) [20], in which the systematic uncertainties largely cancel out, agree with the results in Table II.

For $\mathcal{B}(\chi_{c0}(1P) \to J/\psi e^+e^-)$, the obtained value favorably compares with the average in Table I. The prediction for $\mathcal{B}(\chi_{c0}(1P) \to J/\psi\mu^+\mu^-)$ is also compatible with the upper bound reported in the same Table. For the Dalitz decays of $h_c(1P)$, no result is quoted in Ref. [2]. An analysis by the BESIII Collaboration reports the measurement of the ratio $\mathcal{R} = \frac{\mathcal{B}(h_c(1P) \to \eta_c(1S)e^+e^-)}{\mathcal{B}(h_c(1P) \to \eta_c(1S)\gamma)}$, with result depending on the h_c production mechanism [21]. Two possibilities are considered: h_c producted via $\psi(3686) \to e^+e^-h_c$, which gives $\mathcal{R} = (0.46 \pm 0.12 \pm 0.05) \times 10^{-2}$, and h_c produced through $e^+e^- \to \pi^+\pi^-h_c$, which gives $\mathcal{R} = (0.89 \pm 0.19 \pm 0.09) \times 10^{-2}$. Combining the two results, the average is quoted: $\mathcal{R} = (0.59 \pm 0.10 \pm 0.04) \times 10^{-2}$, where the first error is statistical and the second is systematic. Using the radiative branching fraction in Table I, this corresponds to $\mathcal{B}(h_c(1P) \to \eta_c(1S)e^+e^-) = (3.5 \pm 0.9) \times 10^{-3}$. The prediction in Table II is marginally consistent with this experimental result, which, however, suffers from the method to obtain it.

For the modes $\chi_{c1}(1P) \to J/\psi\mu^+\mu^-$ and $\chi_{c2}(1P) \to J/\psi\mu^+\mu^-$, the BESIII Collaboration has measured the branching fraction, respectively, in four and five bins of q^2, determining in each bin the transition form factor [20]. In Fig. 1, we compare the result obtained using a_{c1}, a_{c2} (magenta regions), and a_c (dark blue regions) to the BESIII measurement (binned cyan regions). The effect of the transition form factor also emerges considering the ratios $\mathcal{R}^{ee}_{J,\gamma} = \frac{\mathcal{B}(\chi_{cJ} \to J/\psi e^+e^-)}{\mathcal{B}(\chi_{cJ} \to J/\psi\gamma)}$. With the expression (17), we obtain $\mathcal{R}^{ee}_{0,\gamma} = 8.4 \times 10^{-3}$, $\mathcal{R}^{ee}_{1,\gamma} = 9.0 \times 10^{-3}$, and $\mathcal{R}^{ee}_{2,\gamma} = 9.2 \times 10^{-3}$, to be compared to the measurements $\mathcal{R}^{ee}_{0,\gamma}|_{\rm exp} = (9.5 \pm 1.9 \pm 0.7) \times 10^{-3}$, $\mathcal{R}^{ee}_{1,\gamma}|_{\rm exp} = (10.1 \pm 0.3 \pm 0.5) \times 10^{-3}$, and $\mathcal{R}^{ee}_{2,\gamma}|_{\rm exp} = (11.3 \pm 0.4 \pm 0.5) \times 10^{-3}$ [22]. For constant TFF, $f(q^2) = 1$, the computed ratios are systematically reduced: $\mathcal{R}^{ee}_{0,\gamma} = 8.2 \times 10^{-3}$, $\mathcal{R}^{ee}_{1,\gamma} = 8.6 \times 10^{-3}$, and $\mathcal{R}^{ee}_{2,\gamma} = 8.8 \times 10^{-3}$.

The $M_{e^+e^-}$ distributions of $\chi_{cJ}(1P) \to \psi(1S)e^+e^-$ have been measured in the full kinematic range for $J = 1, 2$ [22], and recently with higher precision in the low range up to 0.12 GeV for $J = 0, 1, 2$ [23]. Figures 2 and 3 show the comparison of the distributions obtained using Eqs. (1), (17), and (20) (setting a suitable normalization in the

TABLE II. Computed branching fractions of $1P \to 1S$ charmonium Dalitz modes using the TFF in (17) and the pole mass parameter in (20).

$M' \to M$	$\mathcal{B}(M' \to M\mu^+\mu^-)$	$\mathcal{B}(M' \to Me^+e^-)$	$\frac{\mathcal{B}(M' \to M\mu^+\mu^-)}{\mathcal{B}(M' \to Me^+e^-)}$
$\chi_{c0}(1P) \to J/\psi$	$(4.02 \pm 0.26) \times 10^{-6}$	$(1.2 \pm 0.1) \times 10^{-4}$	3.4×10^{-2}
$\chi_{c1}(1P) \to J/\psi$	$(2.47 \pm 0.09) \times 10^{-4}$	$(3.08 \pm 0.12) \times 10^{-3}$	8.0×10^{-2}
$\chi_{c2}(1P) \to J/\psi$	$(1.85 \pm 0.08) \times 10^{-4}$	$(1.80 \pm 0.08) \times 10^{-3}$	10.3×10^{-2}
$h_c(1P) \to \eta_c$	$(8.7 \pm 0.6) \times 10^{-4}$	$(5.9 \pm 0.4) \times 10^{-3}$	14.7×10^{-2}

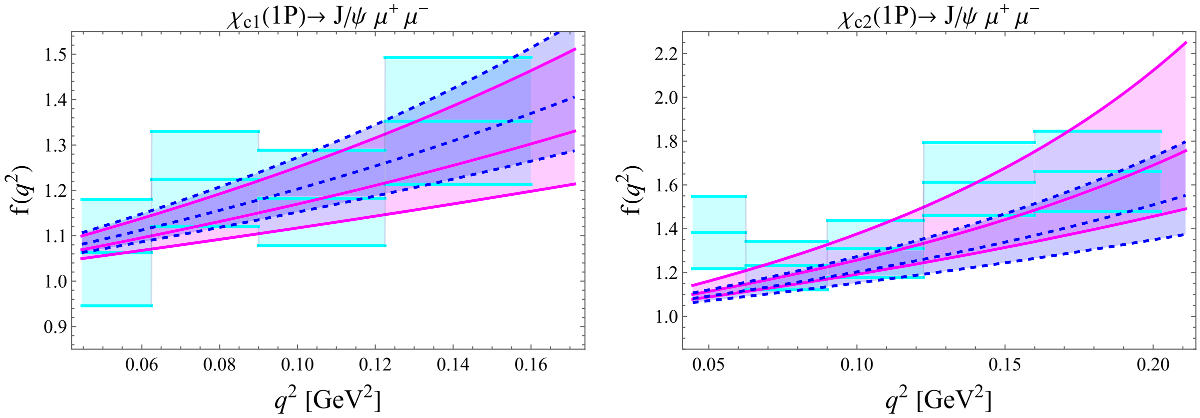

FIG. 1. Transition form factor $f(q^2)$ for $\chi_{c1}(1P) \to J/\psi\mu^+\mu^-$ (left panel) and $\chi_{c2}(1P) \to J/\psi\mu^+\mu^-$ (right panel). The binned cyan regions are the BESIII results [20]. The magenta regions are obtained using Eq. (17) with the values a_{c1} and a_{c2} determined independently for the two modes, and the blue regions are obtained for the common value a_c in (20).

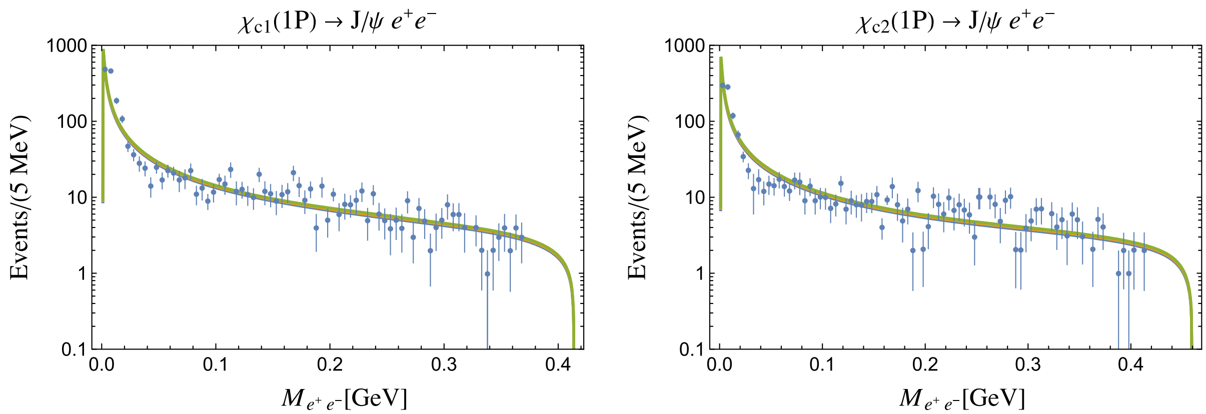

FIG. 2. $M_{e^+e^-}$ distributions for $\chi_{cJ}(1P) \to J/\psi e^+e^-$ ($J = 1, 2$) in the full kinematical range, computed using the TFF in (17) and the pole mass parameter in (20) (continuous line), compared to the BESIII data [22].

various cases) with the measured spectra. Overall agreement is found. The enhancement near the real photon production is clearly observed. In the case of $\chi_{c1}(1P)$ and $\chi_{c2}(1P)$, there is an apparent excess of events in the dielectron mass distribution for low $M_{e^+e^-}$; see Fig. 3. This is a warning that we shall discuss in the last section.

We conclude with a comment on the size of the corrections expected for the predictions based on the heavy quark spin symmetry. Such a comment also applies to the processes analyzed in the following. The breaking of the heavy quark spin symmetry affects the radiative amplitude at zero recoil and the extrapolation in the dilepton invariant mass, which is extended for the dielectron mode to a kinematical range broader than the range of the dimuon mode. A quantitative assessment of the size of such effects must be based on explicit calculations in a QCD based framework, and it is not affordable within the present approach. However, information on the heavy quark spin breaking effects comes from the spectrum of the decaying particles. Using the central values of the masses quoted by PDG, the spin-spin and spin-orbit parameters entering in the hyperfine and fine mass splittings are $\Delta_{SS} \sim -2$ MeV and $\Delta_{LS} \sim 44$ MeV for the $1P$ charmonium quartet, $\Delta_{SS} \sim 0.1$ MeV and $\Delta_{LS} \sim 16.4$ MeV for the $1P$, and $\Delta_{SS} \sim -0.01$ MeV and $\Delta_{LS} \sim 11$ MeV for the $2P$ bottomonium quartet. This amounts to effects of the order 10^{-2} for the $1P$ charmonium and 10^{-3} and 10^{-4} for the $1P$ and $2P$ bottomonium quartets. It is reasonable that the corrections to decay amplitudes at zero recoil are not exceedingly larger; the available data on the radiative widths confirm this. As for the extrapolation in q^2, it is reassuring that the same value of the pole mass parameter a obtained in the dimuon case reproduces the spectrum in the dielectron case in the case where a comparison is possible, $\chi_{c1,2}(1P) \to J/\psi\mu^+\mu^-(e^+e^-)$. This suggests that the ratios quoted in Table II are robust.

B. Charmonium $2S \to 1P$ Dalitz decays

Among the transitions from the $2S$ doublet to the $1P$ quartet, measurements are available for the widths of the

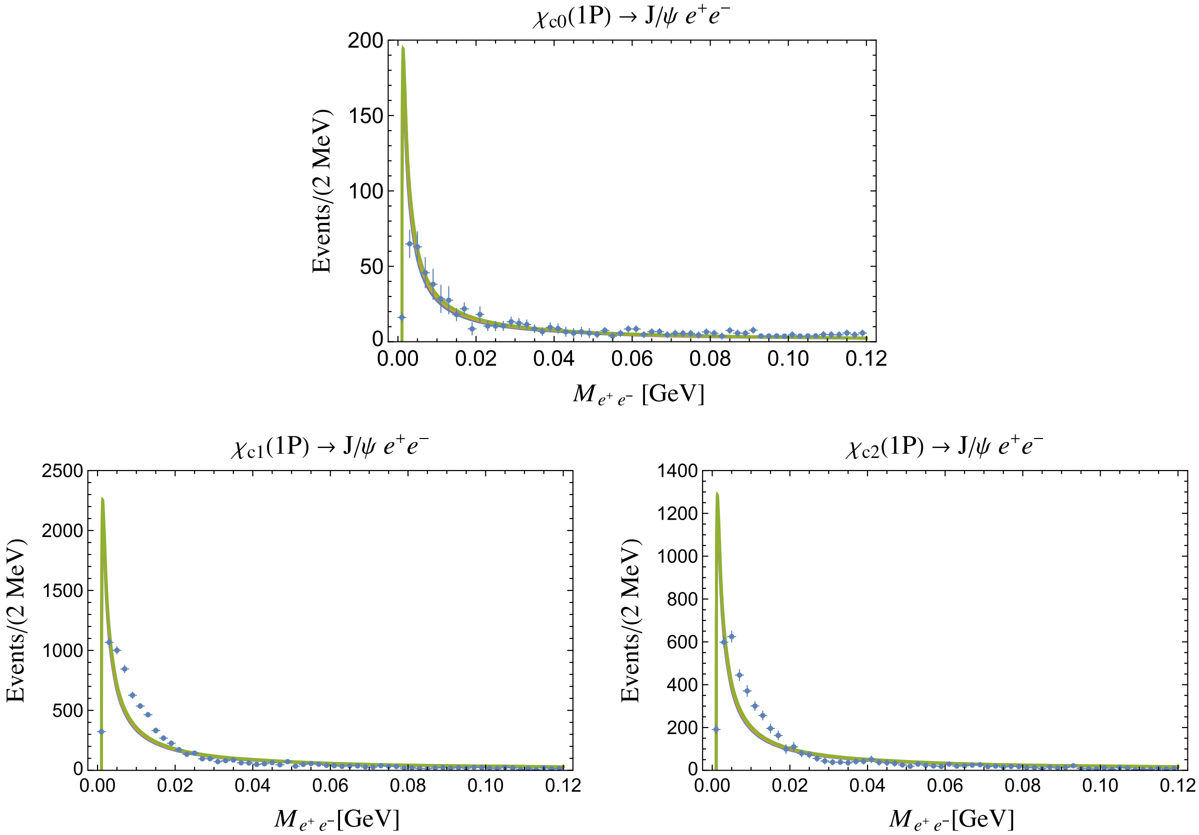

FIG. 3. $M_{e^+e^-}$ distributions for $\chi_{cJ}(1P) \to J/\psi e^+e^-$ ($J = 0$, 1, 2) in the low range of dilepton mass, computed using the TFF in (17) and the pole mass parameter in (20) (continuous line). The dots are the BESIII measurement [23].

decays $\psi(2S) \to \chi_{cJ}\gamma$ and of the Dalitz modes $\psi(2S) \to \chi_{cJ}e^+e^-$ ($J = 0$, 1, 2) in Table I. No data are available for Dalitz decays to muons. The measured $\mathcal{B}(\psi(2S) \to \chi_{cJ}e^+e^-)$ can be used to determine the TFF mass parameter:

$$a_{c,2S} = 0.286^{+0.009}_{-0.001}\ \mathrm{GeV}. \tag{21}$$

The comparison of the $M_{e^+e^-}$ distribution obtained with this TFF, setting a suitable normalization, with the spectra measured by BESIII [22], shown in Fig. 4, supports the statement that the same transition form factor enters in both the modes $\psi(2S) \to \chi_{c1,2}(1P)e^+e^-$. The small value obtained for $a_{c,2S}$ is responsible of the agreement mainly for large dielectron invariant mass.

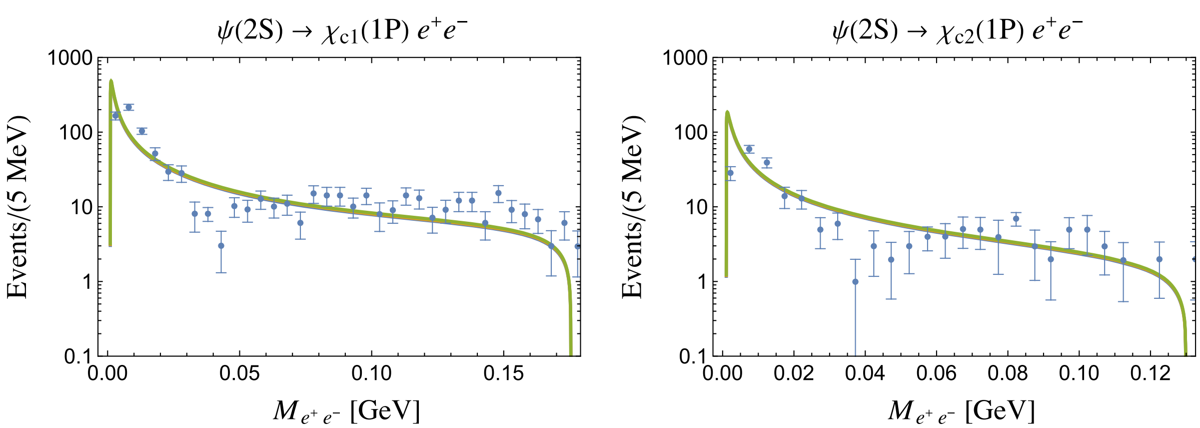

FIG. 4. $M_{e^+e^-}$ distributions of $\psi(2S) \to \chi_{cJ}(1P)e^+e^-$ (for $J = 1$, 2) in the full kinematical range, computed using the TFF in (17) with the parameter in (21) (continuous line), compared to the BESIII data [22].

TABLE III. Branching fractions of charmonium $2S \to 1P$ and $2P \to 1S$ Dalitz decays computed using spin symmetry relations. For $\chi_{c1}(2P)$, see the discussion in the text. For $\chi_{c0}(2P)$ and $h_c(2P)$, the uncertainties of the input data (when available) are too large to obtain predictions.

$M' \to M$	$\mathcal{B}(M' \to M\mu^+\mu^-)$	$\mathcal{B}(M' \to Me^+e^-)$
$\psi(2S) \to \chi_{c0}(1P)$	$(1.51 \pm 0.04) \times 10^{-4}$	$(11.1 \pm 0.3) \times 10^{-4}$
$\psi(2S) \to \chi_{c1}(1P)$	$(2.46 \pm 0.07) \times 10^{-5}$	$(7.6 \pm 0.2) \times 10^{-4}$
$\psi(2S) \to \chi_{c2}(1P)$	$(1.53 \pm 0.04) \times 10^{-4}$	$(6.6 \pm 0.2) \times 10^{-4}$
$\eta_c(2S) \to h_c(1P)$	$(5.7 \pm 0.9) \times 10^{-6}$	$(1.35 \pm 0.2) \times 10^{-5}$
$\chi_{c1}(2P) \to J/\psi$	$(4.2 \pm 1.7) \times 10^{-5}$	$(1.3 \pm 0.5) \times 10^{-4}$
$\chi_{c2}(2P) \to J/\psi$	$(1.6 \pm 0.7) \times 10^{-5}$	$(2.9 \pm 0.9) \times 10^{-5}$

With the parameter (21), we compute the branching fractions in Table III. For $\eta_c(2S)$, no measurement is available. Using the expressions in the Appendix, the HQ spin symmetry relations allowed us to predict $\mathcal{B}(\eta_c(2S) \to h_c(1P)\gamma) = (0.20 \pm 0.03) \times 10^{-2}$ [15]. With this result and the mass parameter in (21), we obtain the predictions for $\mathcal{B}(\eta_c(2S) \to h_c(1P)\mu^+\mu^-)$ and $\mathcal{B}(\eta_c(2S) \to h_c(1P)e^+e^-)$ in Table III.

C. Charmonium $2P \to 1S$ Dalitz decays

The $2P \to 1S$ transitions are of interest since they involve the debated state $\chi_{c1}(3872)$. If $\chi_{c1}(3872)$ is identified with $\chi_{c1}(2P)$, a piece of information comes from the measured $\mathcal{B}(\chi_{c1}(3872) \to J/\psi\gamma)$ in Table I. Exploiting the HQ relations, using meson masses and widths in Ref. [2] and the expressions in the Appendix, this measurement implies[3]

$$\mathcal{B}(\chi_{c2}(2P) \to J/\psi\gamma) = (4.0 \pm 1.8) \times 10^{-4}. \quad (22)$$

In the HQ limit, the TFF mass parameter a is expected to be the same for $\chi_{c1}(2P) \to J/\psi\ell^+\ell^-$ and $\chi_{c2}(2P) \to J/\psi\ell^+\ell^-$. Imposing a conservative bound

$$0.3 \le \frac{\mathcal{B}(\chi_{c2}(2P) \to J/\psi\mu^+\mu^-)}{\mathcal{B}(\chi_{c1}(2P) \to J/\psi\mu^+\mu^-)} \le 1, \quad (23)$$

we obtain

$$a_{c,2P} = 0.826 \text{ GeV}. \quad (24)$$

This allows us to compute the branching fractions of the Dalitz modes $\chi_{c1,2}(2P) \to J/\psi$ reported in Table III. For the $\chi_{c0}(2P)$ and $h_c(2P)$ Dalitz modes, the input data (when available) are too uncertain to derive predictions. In the case of $\chi_{c1}(2P)$ decay, a further contribution to the $\chi_{c1}(2P) \to J/\psi\ell^+\ell^-$ amplitude comes from $\chi_{c1}(2P) \to J/\psi(\rho^0,\omega) \to J/\psi\ell^+\ell^-$. It involves the isospin-violating $\chi_{c1}(2P) \to J/\psi\rho^0$ mode observed for $\chi_{c1}(3872)$, the branching fraction of which is quoted in Ref. [2] and is connected to the tale of the ρ^0 line shape (the intermediate virtual ω is too narrow for providing a relevant effect). To estimate such a contribution, we compute the $\chi_{c1}(2P) \to J/\psi\ell^+\ell^-$ branching fraction taking into account only the ρ^0-exchange amplitude. We use a constant transition form factor and a ρ^0 mass 0.5 MeV away from the nominal value. We obtain results about a factor of 2 smaller than those quoted in Table III, both for the electron and muon mode. This implies that this contribution cannot be neglected, mainly because the relative phase with respect to the internal photon conversion amplitude is not known. A possibility to account for this contribution is to double the errors quoted in Table III. The study of the q^2 distribution would allow us to isolate the vector meson-exchange contribution, since an enhancement is foreseen in the end point q^2 region.

Let us conclude with a comment on the identification of $\chi_{c1}(3872)$ with $\chi_{c1}(2P)$. Our description of a Dalitz decay relies on (1) the radiative width of the parent state, (2) the TFF associated with the process $\chi_{c1}(3872) \to \psi\gamma^*$, and (3) the QED conversion form factor describing the virtual photon decay into a lepton pair. The QED form factor is determined by electrodynamics; it is insensitive to the internal structure of the decaying resonance. Any dependence on the structure enters through the radiative decay amplitude and the TFF.

In our analysis, since experimental radiative branching ratios are used as input, the single Dalitz decay rate does not directly discriminate among different interpretations. Nevertheless, information on the structure is encoded in the pattern of radiative transitions within a heavy–quark spin multiplet: heavy-quark spin symmetry (HQSS) predicts correlations among radiative decay amplitudes of states belonging to the same multiplet and holds for a conventional $\chi_{c1}(2P)$ assignment. In contrast, if the $\chi_{c1}(3872)$ had a dominant molecular or multiquark component, radiative transitions would receive contributions not only from the heavy quark pair but also from other light degrees of freedom. In that case, the HQSS-based correlations among radiative widths would not necessarily hold, and deviations from the predicted multiplet relations can be expected. The alignment of the predictions obtained using HQSS for the radiative decay rates with recent measurements supports the conventional interpretation.

The transition form factor may depend on the structure of the decaying state. However, in the kinematic region relevant for Dalitz decays, the virtual photon invariant mass is restricted to relatively small values. The TFF, which is normalized at $q^2 = 0$, is expected to vary slowly with the photon virtuality. Possible differences between a charmonium configuration, a molecular, a multiquark, or a mixed scenarios could manifest in a different q^2 dependence.

[3]This value updates the result in Ref. [15] due to a slight change of the datum for $\mathcal{B}(\chi_{c1}(3872) \to J/\psi\gamma)$ used as input.

Quantifying such effects requires a dedicated dynamical calculation within a specific model for the internal structure of $\chi_{c1}(3872)$, each one predicting a shape of the form factor. Such an analysis goes beyond the present work, it would be a topic for an investigation focused on the differences between Dalitz decays of conventional and exotic mesons. The measurement of the q^2 distribution in $\chi_{c1}(3872) \to \psi\ell^+\ell^-$ will add information on the underlying transition dynamics, giving in future new elements to discriminate among different interpretations of $\chi_{c1}(3872)$.

D. Bottomonium $1P \to 1S$ and $2P \to 1S$ Dalitz modes

For bottomonium, there are no measurements of χ_{bJ} and h_b Dalitz decay widths. A piece of information has been provided by the LHCb Collaboration with the analysis of $\chi_{b1,2}(1P) \to \Upsilon(1S)\mu^+\mu^-$ and of the analogous modes for $2P$ excitations $\chi_{b1,2}(2P) \to \Upsilon(1S)\mu^+\mu^-$ [24]. The analysis has improved the mass determination of $\chi_{b1,2}(1P,2P)$ with respect to the PDG values: $m_{\chi_{c1}(1P)} = 9892.50 \pm 0.26 \pm 0.10 \pm 0.10$ MeV, $m_{\chi_{c2}(1P)} = 9911.92 \pm 0.29 \pm 0.11 \pm 0.10$ MeV, $m_{\chi_{c1}(2P)} = 10253.97 \pm 0.75 \pm 0.22 \pm 0.09$ MeV, $m_{\chi_{c2}(2P)} = 10269.67 \pm 0.67 \pm 0.22 \pm 0.09$ MeV [the first error is statistical, the second error is systematic, and the third one is from the knowledge of the $\Upsilon(1S)$ mass] [24]. Moreover, yields has been measured from a fit of the $\Upsilon(1S)\mu^+\mu^-$ mass distribution:

$$
\begin{aligned}
N(\chi_{b1}(1P) \to \Upsilon(1S)\mu^+\mu^-) &= 53.6 \pm 7.7, \\
N(\chi_{b2}(1P) \to \Upsilon(1S)\mu^+\mu^-) &= 47.9 \pm 7.4, \\
N(\chi_{b1}(2P) \to \Upsilon(1S)\mu^+\mu^-) &= 51.1 \pm 10.4, \\
N(\chi_{b2}(2P) \to \Upsilon(1S)\mu^+\mu^-) &= 59.3 \pm 10.4. \qquad (25)
\end{aligned}
$$

For each process, the yield N is proportional to the decay branching fraction $\mathcal{B}$ through the relation

$$N = L \times \sigma \times A \times \epsilon \times \mathcal{B}, \qquad (26)$$

where L is the integrated luminosity, A is the acceptance, σ is the production cross section, and ϵ is the reconstruction efficiency. We consider ratios of branching fractions for decaying particles in the same spin multiplet,

$$R_{b,1P} = \frac{\mathcal{B}(\chi_{b2}(1P) \to \Upsilon(1S)\mu^+\mu^-)}{\mathcal{B}(\chi_{b1}(1P) \to \Upsilon(1S)\mu^+\mu^-)} \qquad (27)$$

$$R_{b,2P} = \frac{\mathcal{B}(\chi_{b2}(2P) \to \Upsilon(1S)\mu^+\mu^-)}{\mathcal{B}(\chi_{b1}(2P) \to \Upsilon(1S)\mu^+\mu^-)} \qquad (28)$$

and, invoking spin symmetry, we assume that for the two modes in each ratio (27) and (28) the TFF is the same. The quantities in Eq. (26) depending only on the detector and not on the decaying particle cancel out in the ratios. As for the production cross section, a simple argument assumes that it is proportional to the number of the spin states of the decaying particle. This gives $\sigma(\chi_{b2})/\sigma(\chi_{b1}) \simeq 5/3$. Deviations are expected in particular for production in the low p_T region.[4] Actually, the production pattern of the χ_{bJ} states at hadron colliders may depend on the transverse momentum and on the underlying production mechanism. Studies based on nonrelativistic QCD indicate variations of the relative production rates of the different spin states at the level of tens of percent [25,26]. A systematic uncertainty at this level must be included in the estimates of the Dalitz branching fractions.

Using the simple assumption based on spin states counting, we have

$$R_{b,1P} \simeq \frac{3}{5}\frac{N(\chi_{b2}(1P) \to \Upsilon(1S)\mu^+\mu^-)}{N(\chi_{b1}(1P) \to \Upsilon(1S)\mu^+\mu^-)} = 0.54 \pm 0.11 \qquad (29)$$

$$R_{b,2P} \simeq \frac{3}{5}\frac{N(\chi_{b2}(2P) \to \Upsilon(1S)\mu^+\mu^-)}{N(\chi_{b1}(2P) \to \Upsilon(1S)\mu^+\mu^-)} = 0.70 \pm 0.19. \qquad (30)$$

Requiring that the ratios (29) and (30) are recovered within 2σ constrains each TFF mass parameter a:

$$a_{b,1P} \in [0.48, 1] \text{ GeV}, \qquad a_{b,2P} \in [0.82, 2] \text{ GeV}. \qquad (31)$$

Varying the mass parameter a in (31) produces a correlation between the two modes in each ratio, as shown in Fig. 5. Although the bounds (29) and (30) can be fulfilled for values of $a_{b,1P}$ and $a_{b,2P}$ above the ranges (31), there are no visible differences in the correlation plots since such large values only populate the region of smallest branching fractions.

Using the radiative rates in Table I and setting $a_{b,1P} = 0.74$ GeV and $a_{b,2P} = 1.41$ GeV, we compute the branching ratios of all $1P \to 1S$ and $2P \to 1S$ Dalitz bottomonium decays in Table IV. The branching fractions of the Dalitz decays of $\chi_{b1,2}(2P)$ due to ω-exchanges, obtained using the measured $\mathcal{B}(\chi_{b1,2}(2P) \to Y(1S)\omega)$ [2], turn out to be 2 orders of magnitude smaller than the ones quoted in Table IV. The ω-exchange contribution can be efficiently subtracted in the q^2 distributions. The results in Table IV are within the reach of the present experimental facilities.

IV. SENSITIVITY OF HEAVY QUARKONIUM DALITZ MODES TO A DARK PHOTON

The sensitivity of Dalitz decays of heavy quarkonia to the contribution of a new light vector mediator, such as the dark photon (γ') or U boson, merits investigations. This mediator is a prediction of models extending the Standard Model with an additional $U(1)'$ gauge symmetry.

The proposed dark photon has been connected to anomalies reported by experiments utilizing the ATOMKI

[4]We thank I. Belyaev for pointing this out to us.

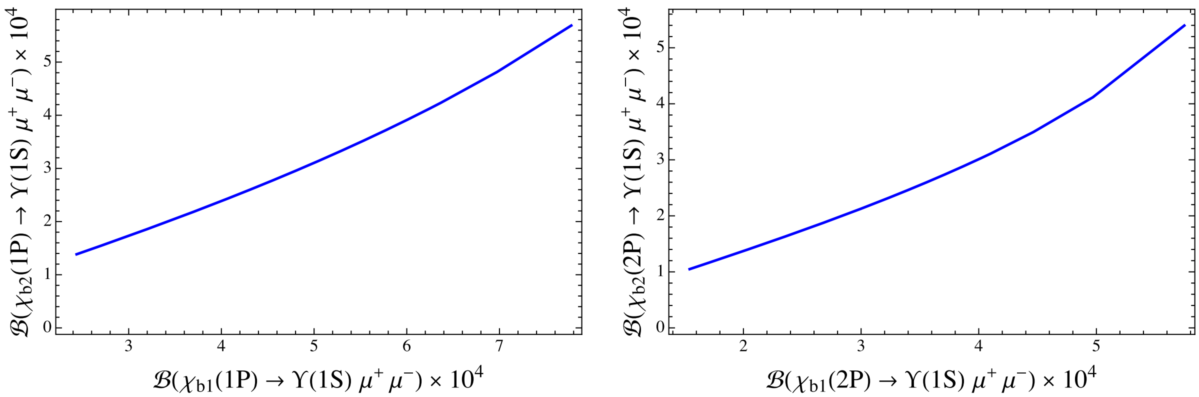

FIG. 5. Correlation between $\mathcal{B}(\chi_{b2}(1P) \to \Upsilon(1S)\mu^+\mu^-)$ and $\mathcal{B}(\chi_{b1}(1P) \to \Upsilon(1S)\mu^+\mu^-)$ (left panel) and between $\mathcal{B}(\chi_{b2}(2P) \to \Upsilon(1S)\mu^+\mu^-)$ and $\mathcal{B}(\chi_{b1}(2P) \to \Upsilon(1S)\mu^+\mu^-)$ (right panel), obtained varying the TFF parameters $a_{b,1P}$ and $a_{b,2P}$ in the ranges in Eq. (31).

spectrometer [7,27,28]. Specifically, an excess of events was observed in the distribution of e^+e^- pair opening angle at large angles, resulting from the internal conversion in nuclear deexcitation of ^{8}Be, ^{4}He, and ^{12}C. The observation was confirmed by the VINATOM experiment [29]. In contrast, other searches, as the MEG II experiment, have neither confirmed [30] nor excluded the anomaly [31]. Proposed explanations of the ATOMKI anomaly require a new boson, often designed $X(17)$, with an approximate mass of $m_X \simeq 17$ MeV.

Excluding other possibilities, the $X(17)$ particle could be the $U(1)'$ gauge mediator with feeble interaction with SM particles [32,33]. The interaction of this mediator (the A' field) with ordinary fermions is described by a Lagrangian analogous to the electromagnetic Lagrangian,

$$\mathcal{L}_X = -\sum_f (e k_f J^\mu_f A'_\mu), \tag{32}$$

where $J^\mu_f = \bar{f}\gamma^\mu f$ is the fermion current. The dimensionless parameters k_f govern the coupling strengths and are specified as $k_\ell = \epsilon_\ell$ for leptons (ϵ_ℓ is the lepton specific coupling) and $k_q = e_q \epsilon_q$ for quarks (e_q is the quark electric charge and ϵ_q the quark specific coupling). Furthermore, the new mediator can interact with the Standard Model electromagnetic field via the kinetic mixing

$$\mathcal{L}_{\rm mix} = -\frac{\epsilon}{2} F'_{\mu\nu} F^{\mu\nu}, \tag{33}$$

with ϵ the mixing parameter governing the interaction [34,35]. A small width is expected for light γ', with mass below 1 GeV [36–38]. Such a light mediator has been searched at beam dump experiments [39,40], fixed target facilities [41–48], and colliders [49–60] including PADME experiment at the Frascati INFN National Laboratories [61,62]. Methods designed for searching the ATOMKI $X(17)$ signal have been proposed [63–66]. Constraints for the parameter space have been derived, with the conclusion that the results of the ATOMKI experiment are compatible with the e^+e^- coupling ϵ_e in the range $\epsilon_e \in [0.2, 1.4] \times 10^{-3}$ [67].

Charm decays are important processes where to investigate $X(17)(\gamma')$ [68–73]. If produced in processes such as $M' \to M\gamma'$ followed by $\gamma' \to \ell^+\ell^-$, the γ' contribution would modify the Dalitz decay width and the dilepton invariant mass distribution. The largest effect would be close to $m_{\gamma'}$ if the mass is in the q^2 kinematical range.

Experimental studies have been carried out on the channels $J/\psi \to \eta^{(\prime)}\gamma'(e^+e^-)$ [53,54] and $\chi_{cJ} \to J/\psi\gamma'(e^+e^-)$ (with $J = 0, 1, 2$) [23]. Here, we analyze the role of $X(17)(\gamma')$ in the Dalitz decays $\chi_{c1,2}(1P) \to J/\psi\ell^+\ell^-$, with $\ell = \mu, e$, for which the most precise data are available. The contribution of a new vector mediator of mass m_X and width Γ_X modifies Eq. (6),

$$F_{\rm Dark}(q^2) = F_{\rm QED}(q^2) \times \left| 1 + e^{i\phi}\epsilon_c\epsilon_e \frac{q^2}{q^2 - m_X^2 + i m_X \Gamma_X} \right|^2, \tag{34}$$

TABLE IV. Branching fractions of bottomonium $1P \to 1S$ and $2P \to 1S$ Dalitz decays computed using the TFF mass parameters $a_{b,1P} = 0.74$ GeV and $a_{b,2P} = 1.41$ GeV.

$M' \to M$	$\mathcal{B}(M' \to M\mu^+\mu^-)$	$\mathcal{B}(M' \to Me^+e^-)$
$\chi_{b0}(1P) \to \Upsilon(1S)$	$(1.3 \pm 0.2) \times 10^{-5}$	$(1.7 \pm 0.25) \times 10^{-4}$
$\chi_{b1}(1P) \to \Upsilon(1S)$	$(3.0 \pm 0.2) \times 10^{-4}$	$(3.2 \pm 0.2) \times 10^{-3}$
$\chi_{b2}(1P) \to \Upsilon(1S)$	$(1.7 \pm 0.1) \times 10^{-4}$	$(1.7 \pm 0.1) \times 10^{-3}$
$h_b(1P) \to \eta_b(1S)$	$(6.5 \pm 0.8) \times 10^{-4}$	$(5.6 \pm 0.6) \times 10^{-3}$
$\chi_{b0}(2P) \to \Upsilon(1S)$	$(6.4 \pm 2.9) \times 10^{-6}$	$(3.8 \pm 1.7) \times 10^{-5}$
$\chi_{b1}(2P) \to \Upsilon(1S)$	$(1.75 \pm 0.2) \times 10^{-4}$	$(1.0 \pm 0.1) \times 10^{-3}$
$\chi_{b2}(2P) \to \Upsilon(1S)$	$(1.2 \pm 0.15) \times 10^{-4}$	$(6.7 \pm 0.8) \times 10^{-4}$
$h_b(2P) \to \eta_b(1S)$	$(4.35 \pm 1.0) \times 10^{-4}$	$(2.25 \pm 0.5) \times 10^{-3}$

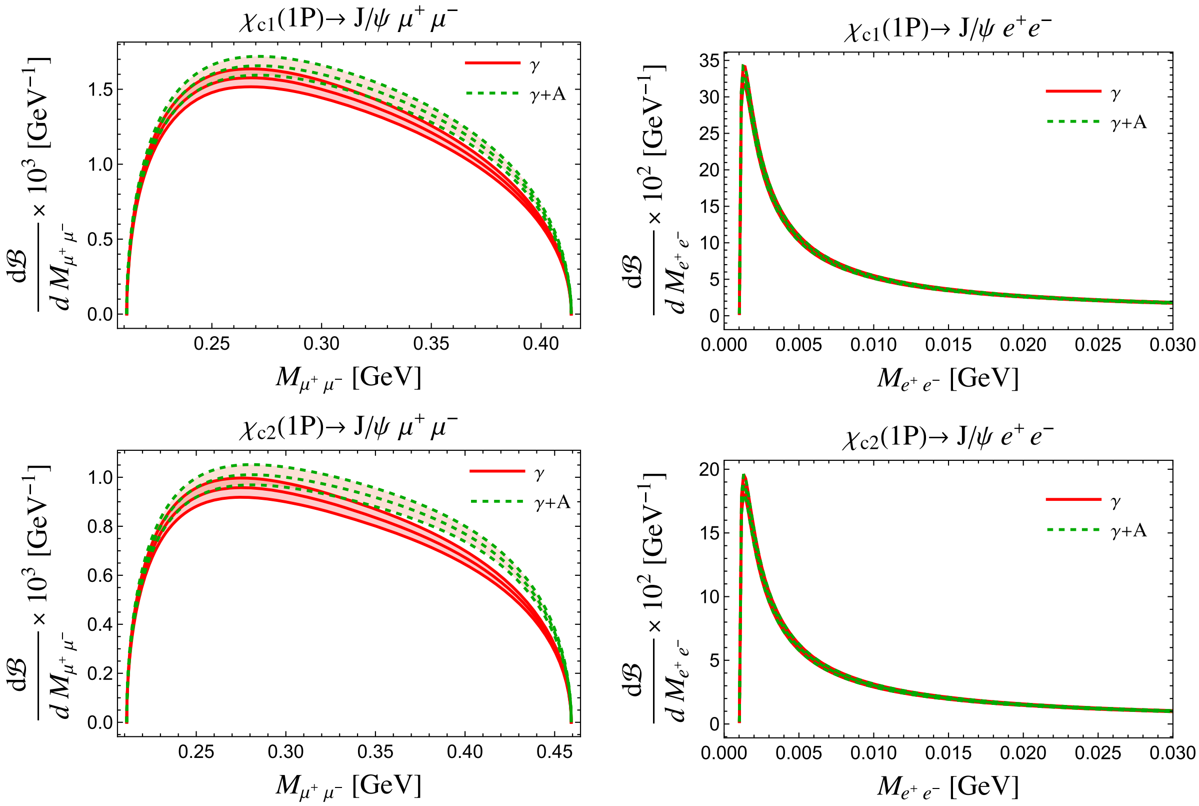

FIG. 6. Dilepton distributions with (red continuous lines) and without (green dashed lines) the dark photon contribution in $\chi_{c1}(1P) \to J/\psi\ell^+\ell^-$ (top panels) and $\chi_{c2}(1P) \to J/\psi\ell^+\ell^-$ (bottom panels). The left plots refer to the muon channel, and the right ones refer to the electron channel.

with ϕ a phase between the photon and dark photon amplitudes. We fit $\mathcal{B}(\chi_{c1}(1P) \to J/\psi e^+e^-)$ and $\mathcal{B}(\chi_{c1}(1P) \to J/\psi\mu^+\mu^-)$ to determine the parameters in Eq. (34) together with TFF mass parameter. The results are used to compute the χ_{c2} decay rate. We set $m_X = 17$ MeV and $\epsilon_e = 1.4 \times 10^{-3}$ at the upper edge of the range obtained in Ref. [67]. For Γ_X, we choose the experimental resolution in the variable $M_{e^+e^-}$ quoted in Ref. [23]: $\Gamma_X \sim 2$ MeV. We vary ϵ_c in a range up to 10^{-2}, considering the upper bound $\epsilon_c < 1.2 \times 10^{-2}$ at 90% C.L. obtained in Ref. [23]. The experimental branching fractions require $\phi = \pi$. The best fit produces a set of pairs (a, ϵ_c), with a benchmark point

$$a = 0.71\ \text{GeV}, \qquad \epsilon_c = 3.2 \times 10^{-3}. \tag{35}$$

The inclusion of the dark photon contribution modifies the preferred value of the mass parameter a in the transition form factor. After having verified that at the benchmark point the Dalitz branching fractions to electrons and muons of the partner state χ_{c2} are obtained, we analyze the dilepton distributions for $\ell = e,\ \mu$; they are displayed in Fig. 6. The impact on the dilepton distribution is small, even though non-negligible. A similar effect is found in the $\chi_{c2} \to J/\psi\ell^+\ell^-$ distributions, shown in the same figure. These results are an indication of the kind of precision requested to display a dark photon effect. Since the deviations are related in all modes, the sensitivity to the new contribution is enhanced if the decays are analyzed altogether.

It would be tempting to attribute the excess of events observed at low values of $M_{e^+e^-}$ for χ_{c1} and χ_{c2}, as displayed in Fig. 3, to a non-Standard-Model contribution. Arguments disfavoring this interpretation include the lack of the related deviation in the case of χ_{c0}, the broad shape of the signal, and that a deviation of this size would necessitate a very large value of the coupling ϵ_c. The full Monte Carlo simulation of the Dalitz processes described in Ref. [23] does not report deviations with respect to the measurements. These arguments induce us to refrain considering the excess as significant. Nevertheless, the warning message should be kept, these modes warrant continued attention.

V. CONCLUSIONS

We have analyzed a set of charmonium and bottomonium Dalitz processes, organized in classes where the decaying mesons belong to the same spin multiplet and also the produced states are comprised in the same spin multiplet. This organization has allowed us to exploit the heavy quark spin symmetry, establishing relations among different modes. The connection with the radiative processes has been systematically used, while the transition form factors have been determined using measurements. A remarkable overall agreement is found between the computed branching fractions and dilepton mass distributions with existing measurements. Predictions have been provided for many unobserved modes. The predicted rates are within the reach of the present experimental facilities. We have also investigated the sensitivity of two charmonium Dalitz processes to a dark photon contribution.

Note added—Recently, the decay $\chi_{c1}(3872) \to J/\psi\mu^+\mu^-$ has been observed by the LHCb Collaboration [74]. The measured branching fraction is consistent with the value reported in this study.

ACKNOWLEDGMENTS

We thank G. Roselli for collaboration in the analysis of radiative heavy quarkonium decays in Ref. [15]. We are grateful to I. Belyaev, M. Buonsante, M. Needham, and M. Pappagallo for discussions. This work has been carried out within the project (Iniziativa Specifica): Precision Studies for Fundamental Interactions (SPIF) of Istituto Nazionale di Fisica Nucleare (INFN).

DATA AVAILABILITY

The data that support the findings of this article are openly available [75].

APPENDIX: RADIATIVE DECAY WIDTHS OF HEAVY QUARKONIUM

We collect the expressions of the widths of electric dipole decays described by the effective Lagrangian (11) [15]. For a quarkonium state, the spectroscopic notation $n^{2s+1}L_J$ is adopted, with n the radial number, L the orbital angular momentum, s the spin of the quark pair, and J the total spin:

$$\Gamma(n^3P_J \to m^3S_1\gamma) = \frac{(\delta_Q^{nPmS})^2}{3\pi} k_\gamma^3 \frac{M_{S_1}}{M_{P_J}} \tag{A1}$$

$$\Gamma(n^1P_1 \to m^1S_0\gamma) = \frac{(\delta_Q^{nPmS})^2}{3\pi} k_\gamma^3 \frac{M_{S_0}}{M_{P_1}} \tag{A2}$$

$$\Gamma(m^3S_1 \to n^3P_J\gamma) = (2J+1)\frac{(\delta_Q^{nPmS})^2}{9\pi} k_\gamma^3 \frac{M_{P_J}}{M_{S_1}} \tag{A3}$$

$$\Gamma(m^1S_0 \to n^1P_1\gamma) = \frac{(\delta_Q^{nPmS})^2}{\pi} k_\gamma^3 \frac{M_{P_1}}{M_{S_0}}. \tag{A4}$$

M_i are the quarkonium masses, and k_γ is the photon energy. Because of the heavy quark spin symmetry, the same coupling δ_Q^{nPmS} governs all channels. The width of the magnetic dipole decay described by the effective Lagrangian (16) reads

$$\Gamma(n^3S_1 \to m^1S_0\gamma) = \frac{4(\delta_Q^{nSmS})^2}{3\pi} k_\gamma^3 \frac{M_{S_0}}{M_{S_1}}. \tag{A5}$$

[1] R. H. Dalitz, On an alternative decay process for the neutral pi-meson, Letters to the Editor, Proc. Phys. Soc. London Sect. A **64**, 667 (1951).

[2] S. Navas *et al.* (Particle Data Group), Review of particle physics, Phys. Rev. D **110**, 030001 (2024).

[3] L. G. Landsberg, Electromagnetic decays of light mesons, Phys. Rep. **128**, 301 (1985).

[4] A. Faessler, C. Fuchs, and M. I. Krivoruchenko, Dilepton spectra from decays of light unflavored mesons, Phys. Rev. C **61**, 035206 (2000).

[5] N. Isgur and M. B. Wise, Spectroscopy with heavy quark symmetry, Phys. Rev. Lett. **66**, 1130 (1991).

[6] M. Neubert, Heavy quark symmetry, Phys. Rep. **245**, 259 (1994).

[7] A. J. Krasznahorkay *et al.*, Observation of anomalous internal pair creation in Be8: A possible indication of a light, neutral boson, Phys. Rev. Lett. **116**, 042501 (2016).

[8] A. V. Luchinsky, Muon pair production in radiative decays of heavy quarkonia, Mod. Phys. Lett. A **33**, 1850001 (2017).

[9] P. Colangelo, F. De Fazio, F. Loparco, and N. Losacco, Dalitz decays $D_{sJ}^{(*)} \to D_s^{(*)}\ell^+\ell^-$, Phys. Rev. D **108**, 074027 (2023).

[10] B. A. Thacker and G. P. Lepage, Heavy quark bound states in lattice QCD, Phys. Rev. D **43**, 196 (1991).

[11] E. E. Jenkins, M. E. Luke, A. V. Manohar, and M. J. Savage, Semileptonic B_c decay and heavy quark spin symmetry, Nucl. Phys. **B390**, 463 (1993).

[12] R. Casalbuoni, A. Deandrea, N. Di Bartolomeo, R. Gatto, F. Feruglio, and G. Nardulli, Phenomenology of heavy meson chiral Lagrangians, Phys. Rep. **281**, 145 (1997).

[13] R. Casalbuoni, A. Deandrea, N. Di Bartolomeo, R. Gatto, F. Feruglio, and G. Nardulli, Effective Lagrangian for quarkonia and light mesons in a soft-exchange-approximation, Phys. Lett. B **302**, 95 (1993).

[14] F. De Fazio, Radiative transitions of heavy quarkonium states, Phys. Rev. D **79**, 054015 (2009); **83**, 099901(E) (2011).

[15] P. Colangelo, F. De Fazio, and G. Roselli, Charming case of X(3872) and $\chi_{c1}(2P)$, Phys. Rev. D **111**, 074014 (2025).

[16] P. L. Cho and H. Georgi, Electromagnetic interactions in heavy hadron chiral theory, Phys. Lett. B **296**, 408 (1992); **300**, 410(E) (1993).

[17] D. Bečirević, R. Di Palma, R. Frezzotti, G. Gagliardi, V. Lubicz, F. Sanfilippo, and N. Tantalo, Lattice QCD determination of the radiative decay rates $h_c \to \eta_c\gamma$ and $h_b \to \eta_b\gamma$, Phys. Rev. D **112**, 034505 (2025).

[18] D. Bečirević, R. Di Palma, R. Frezzotti, G. Gagliardi, V. Lubicz, F. Sanfilippo, and N. Tantalo, Lattice QCD study of the $\chi_{c1} \to J/\psi\gamma$ decay, Phys. Lett. B **868**, 139811 (2025).

[19] X.-H. Wang, Y. Jiang, T. Wang, X.-Z. Tan, G. Li, and G.-L. Wang, Study of the dilepton electromagnetic decays of $\chi_{cJ}(1P)$, Eur. Phys. J. C **79**, 997 (2019).

[20] M. Ablikim *et al.* (BESIII Collaboration), Study of electromagnetic Dalitz decays $\chi_{cJ} \to \mu^+\mu^- J/\psi$, Phys. Rev. D **99**, 051101 (2019).

[21] M. Ablikim *et al.* (BESIII Collaboration), Observation of the electromagnetic Dalitz transition $h_c \to e^+e^-\eta_c$, Phys. Rev. D **110**, L111101 (2024).

[22] M. Ablikim *et al.* (BESIII Collaboration), Observation of $\psi(3686) \to e^+e^-\chi_{cJ}$ and $\chi_{cJ} \to e^+e^- J/\psi$, Phys. Rev. Lett. **118**, 221802 (2017).

[23] M. Ablikim *et al.* (BESIII Collaboration), Search for a hypothetical gauge boson and dark photons in charmonium transitions, Phys. Rev. D **113**, 032009 (2026).

[24] R. Aaij *et al.* (LHCb Collaboration), Observation of muonic Dalitz decays of χ_b mesons and precise spectroscopy of hidden-beauty states, J. High Energy Phys. 10 (2024) 122.

[25] H. Han, Y.-Q. Ma, C. Meng, H.-S. Shao, Y.-J. Zhang, and K.-T. Chao, $\Upsilon(nS)$ and $\chi_b(nP)$ production at hadron colliders in nonrelativistic QCD, Phys. Rev. D **94**, 014028 (2016).

[26] S. S. Biswal, M. Mohanty, and K. Sridhar, Bottomonia production in modified NRQCD, J. Subatomic Part. Cosmol. **3**, 100026 (2025).

[27] A. J. Krasznahorkay, M. Csatlós, L. Csige, J. Gulyás, A. Krasznahorkay, B. M. Nyakó, I. Rajta, J. Timár, I. Vajda, and N. J. Sas, New anomaly observed in He4 supports the existence of the hypothetical X17 particle, Phys. Rev. C **104**, 044003 (2021).

[28] A. J. Krasznahorkay *et al.*, New anomaly observed in C12 supports the existence and the vector character of the hypothetical X17 boson, Phys. Rev. C **106**, L061601 (2022).

[29] T. T. Anh *et al.*, Checking the ^{8}Be anomaly with a two-arm electron positron pair spectrometer, Universe **10**, 168 (2024).

[30] K. Afanaciev *et al.* (MEG II Collaboration), Search for the X17 particle in $^7\mathrm{Li}(\mathrm{p},\mathrm{e}^+\mathrm{e}^-)^8\mathrm{Be}$ processes with the MEG II detector, Eur. Phys. J. C **85**, 763 (2025).

[31] D. Barducci, D. Germani, M. Nardecchia, S. Scacco, and C. Toni, On the Atomki nuclear anomaly after the MEG-II result, J. High Energy Phys. 04 (2025) 035.

[32] M. Fabbrichesi, E. Gabrielli, and G. Lanfranchi, The dark photon, in *The Physics of the Dark Photon: A Primer* (Springer, Cham, 2021).

[33] D. S. M. Alves *et al.*, Shedding light on X17: Community report, Eur. Phys. J. C **83**, 230 (2023).

[34] P. Fayet, Effects of the spin 1 partner of the Goldstino (Gravitino) on neutral current phenomenology, Phys. Lett. **95B**, 285 (1980).

[35] B. Holdom, Two U(1)'s and Epsilon charge shifts, Phys. Lett. **166B**, 196 (1986).

[36] J. D. Bjorken, R. Essig, P. Schuster, and N. Toro, New fixed-target experiments to search for dark gauge forces, Phys. Rev. D **80**, 075018 (2009).

[37] B. Batell, M. Pospelov, and A. Ritz, Probing a secluded U(1) at B-factories, Phys. Rev. D **79**, 115008 (2009).

[38] M. Reece and L.-T. Wang, Searching for the light dark gauge boson in GeV-scale experiments, J. High Energy Phys. 07 (2009) 051.

[39] E. M. Riordan *et al.*, A search for short lived axions in an electron beam dump experiment, Phys. Rev. Lett. **59**, 755 (1987).

[40] A. Bross, M. Crisler, S. H. Pordes, J. Volk, S. Errede, and J. Wrbanek, A search for shortlived particles produced in an electron beam dump, Phys. Rev. Lett. **67**, 2942 (1991).

[41] S. Abrahamyan *et al.* (APEX Collaboration), Search for a new gauge boson in electron-nucleus fixed-target scattering by the APEX Experiment, Phys. Rev. Lett. **107**, 191804 (2011).

[42] G. Agakishiev *et al.* (HADES Collaboration), Searching a dark photon with HADES, Phys. Lett. B **731**, 265 (2014).

[43] H. Merkel *et al.*, Search at the Mainz microtron for light massive gauge bosons relevant for the Muon g-2 anomaly, Phys. Rev. Lett. **112**, 221802 (2014).

[44] J. R. Batley *et al.* (NA48/2 Collaboration), Search for the dark photon in π^0 decays, Phys. Lett. B **746**, 178 (2015).

[45] E. Cortina Gil *et al.* (NA62 Collaboration), Search for production of an invisible dark photon in π^0 decays, J. High Energy Phys. 05 (2019) 182.

[46] E. Cortina Gil *et al.* (NA62 Collaboration), Search for K^+ decays into the $\pi^+e^+e^-e^+e^-$ final state, Phys. Lett. B **846**, 138193 (2023).

[47] D. Banerjee *et al.* (NA64 Collaboration), Search for a hypothetical 16.7 MeV gauge boson and dark photons in the NA64 experiment at CERN, Phys. Rev. Lett. **120**, 231802 (2018).

[48] Y. M. Andreev *et al.* (NA64 Collaboration), Search for light dark matter with NA64 at CERN, Phys. Rev. Lett. **131**, 161801 (2023).

[49] G. Abbiendi *et al.* (OPAL Collaboration), Multiphoton production in e^+e^- collisions at $\sqrt{s} = 181$–209 GeV, Eur. Phys. J. C **26**, 331–344 (2003).

[50] A. Adare *et al.* (PHENIX Collaboration), Search for dark photons from neutral meson decays in $p+p$ and $d+$ Au collisions at $\sqrt{s_{NN}} = 200$ GeV, Phys. Rev. C **91**, 031901 (2015).

[51] J. P. Lees *et al.* (*BABAR* Collaboration), Search for a dark photon in e^+e^- collisions at *BABAR*, Phys. Rev. Lett. **113**, 201801 (2014).

[52] M. Ablikim *et al.* (BESIII Collaboration), Dark photon search in the mass range between 1.5 and 3.4 GeV/c^2, Phys. Lett. B **774**, 252 (2017).

[53] M. Ablikim *et al.* (BESIII Collaboration), Measurement of $\mathcal{B}(J/\psi \to \eta' e^+e^-)$ and search for a dark photon, Phys. Rev. D **99**, 012013 (2019).

[54] M. Ablikim *et al.* (BESIII Collaboration), Study of the Dalitz decay $J/\psi \to e^+e^-\eta$, Phys. Rev. D **99**, 012006 (2019); **104**, 099901(E) (2021).

[55] A. Anastasi *et al.*, Limit on the production of a low-mass vector boson in $\mathrm{e^+e^-} \to \mathrm{U}\gamma$, $\mathrm{U} \to \mathrm{e^+e^-}$ with the KLOE experiment, Phys. Lett. B **750**, 633 (2015).

[56] A. Anastasi *et al.* (KLOE-2 Collaboration), Combined limit on the production of a light gauge boson decaying into $\mu^+\mu^-$ and $\pi^+\pi^-$, Phys. Lett. B **784**, 336 (2018).

[57] R. Aaij *et al.* (LHCb Collaboration), Search for dark photons produced in 13 TeV pp collisions, Phys. Rev. Lett. **120**, 061801 (2018).

[58] F. Abudinén *et al.* (Belle-II Collaboration), Search for a dark photon and an invisible dark Higgs boson in $\mu + \mu-$ and missing energy final states with the Belle II experiment, Phys. Rev. Lett. **130**, 071804 (2023).

[59] G. Aad *et al.* (ATLAS Collaboration), Search for dark photons from Higgs boson decays via ZH production with a photon plus missing transverse momentum signature from pp collisions at $\sqrt{s} = 13$ TeV with the ATLAS detector, J. High Energy Phys. 07 (2023) 133.

[60] A. Hayrapetyan *et al.* (CMS Collaboration), Dark sector searches with the CMS experiment, Phys. Rep. **1115**, 448 (2025).

[61] L. Darmé, M. Mancini, E. Nardi, and M. Raggi, Resonant search for the X17 boson at PADME, Phys. Rev. D **106**, 115036 (2022).

[62] F. Bossi *et al.* (PADME Collaboration), Search for a new 17 MeV resonance via e^+e^- annihilation with the PADME experiment, J. High Energy Phys. 11 (2025) 007.

[63] J. Elam *et al.* (REDTOP Collaboration), The REDTOP experiment: Rare η/η' decays to probe new physics, arXiv:2203.07651.

[64] M. Hostert and M. Pospelov, Pion decay constraints on exotic 17 MeV vector bosons, Phys. Rev. D **108**, 055011 (2023).

[65] B. Dutta, B.-S. Hu, W.-C. Huang, and R. G. Van de Water, Novel approach to Investigate ATOMKI anomaly using coherent CAPTAIN-Mills detectors, Phys. Rev. Lett. **135**, 011801 (2025).

[66] C. Gustavino, X17: Status and perspectives, Universe **10**, 285 (2024).

[67] J. L. Feng, B. Fornal, I. Galon, S. Gardner, J. Smolinsky, T. M. P. Tait, and P. Tanedo, Protophobic fifth-force interpretation of the observed anomaly in ^{8}Be nuclear transitions, Phys. Rev. Lett. **117**, 071803 (2016).

[68] H.-B. Li and T. Luo, Probing Dark force at BES-III/BEPCII, Phys. Lett. B **686**, 249 (2010).

[69] J. Fu, H.-B. Li, X. Qin, and M.-Z. Yang, Study of the electromagnetic transitions $J/\psi \to P\ell^+\ell^-$ and probe dark photon, Mod. Phys. Lett. A **27**, 1250223 (2012).

[70] K. Ban, Y. Jho, Y. Kwon, S. C. Park, S. Park, and P.-Y. Tseng, Search for new light vector boson using J/Ψ at BESIII and Belle II, J. High Energy Phys. 04 (2021) 091.

[71] G. L. Castro and N. Quintero, Tests of the Atomki anomaly in lepton pair decays of heavy mesons, Phys. Rev. D **103**, 093002 (2021).

[72] F.-F. Lee, L. T. T. Uyen, and G.-L. Lin, Testing the hypothesis of vector X17 boson by D meson, Charmonium, and ϕ meson decays, arXiv:2501.13530.

[73] C.-T. Tran, M. A. Ivanov, and A.-T. T. Nguyen, Probing the ATOMKI X17 vector boson using Dalitz decays $V \to Pe^+e^-$, Chin. Phys. **49**, 113105 (2025).

[74] R. Aaij *et al.* (LHCb Collaboration), Observation of the decay $\chi_{c1}(3872) \to J/\Psi\mu^+\mu^-$, arXiv:2601.20790.

[75] https://github.com/picolangelo/files/tree/DN14208.